Supporting Information

Fluorinated Covalent-Organic Framework-Based Quasi-Solid Electrolyte Enable Low-Temperature Lithium-ion Battery

Xin Zhang,‡ Honghong Yang,‡ Chuanbao Jiao, Nan Zhang, Zhe Yang, Xiaomin Kang* and Zhiliang Liu*

College of Chemistry and Chemical Engineering, Inner Mongolia University, Hohhot, 010021, PR China.

E-mail: kangxm@imu.edu.cn, cezlliu@imu.edu.cn

‡ These authors contributed equally to this work.

Table of Contents

and the capacity of 0.1 mAh cm^{-2}, respectively.

19.Fig. S19. SEM images of Li foil from Li symmetric cells with COF-$TA_{0.5}TF_{0.5}$ after the lithium plating/stripping at varying current densities, the capacities and temperatures.

20.Fig.e S20. XPS survey spectrum of COF-$TA_{0.5}TF_{0.5}$; the XPS fitting plot of COF-$TA_{0.5}TF_{0.5}$ after the lithium plating/stripping at the current density of 0.2 mA cm^{-2} and the capacity of 0.2 mAh cm^{-2} for Li 1s and F 1s, respectively.

21.Fig. S21. Charge and discharge voltage profiles of COF-$TA_{0.5}TF_{0.5}$ at different rates; Rate performance of QSSE with COF-$TA_{0.5}TF_{0.5}$.

22.Fig. S22. Photographs showing the bulb being lit by LFP|COF-$TA_{0.5}TF_{0.5}$|Li at room temperature and −40 °C.

23.Fig. S23. Calculated mean square displacement (MSD) of Li^+ in electrolytes as a function of the simulation time.

24.Table S1. ICP-OES results of COF-TA, COF-$TA_{0.5}TF_{0.5}$ and COF-TF.

25.Table S2. The ionic conductivity summery of COF-TA, COF-TF, COF-$TA_{0.75}TF_{0.25}$, COF-$TA_{0.67}TF_{0.33}$, COF-$TA_{0.5}TF_{0.5}$, COF-$TA_{0.33}TF_{0.67}$, COF-$TA_{0.25}TF_{0.75}$ at different temperatures.

26.Table S3. The Li^+ conductivity comparison between COF-$TA_{0.5}TF_{0.5}$ and reported work previously in wide temperature range.

27.Table S4. The cycling performances comparison between COF-$TA_{0.5}TF_{0.5}$ and other similar COF-based electrolytes reported previously.

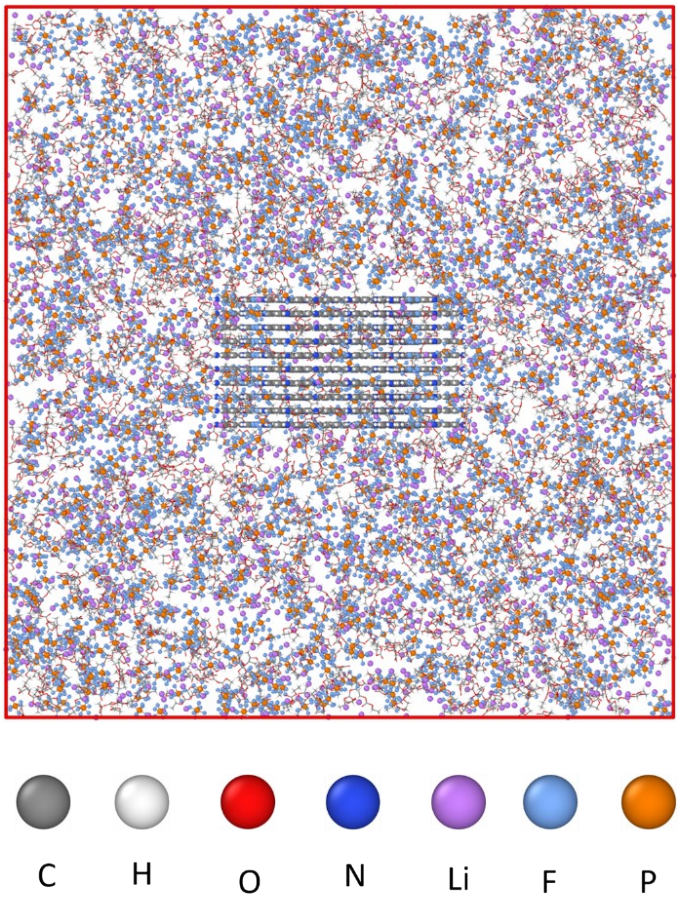

Fig. S1. Simulation model of COF-$TA_{0.5}TF_{0.5}$ QSSE.

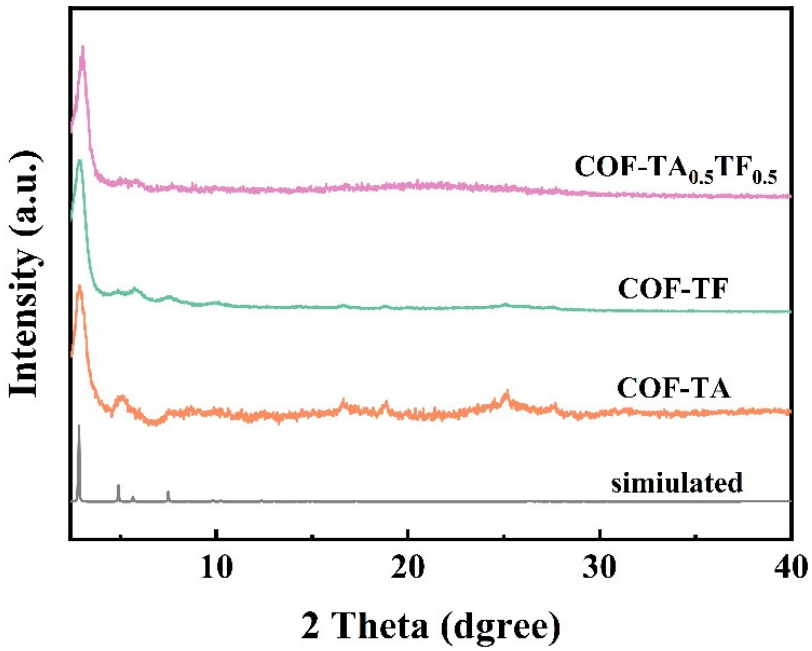

Fig. S2. PXRD patterns of COF-TA, COF-TF and COF-$TA_{0.5}TF_{0.5}$ match well with that of simulated ones.

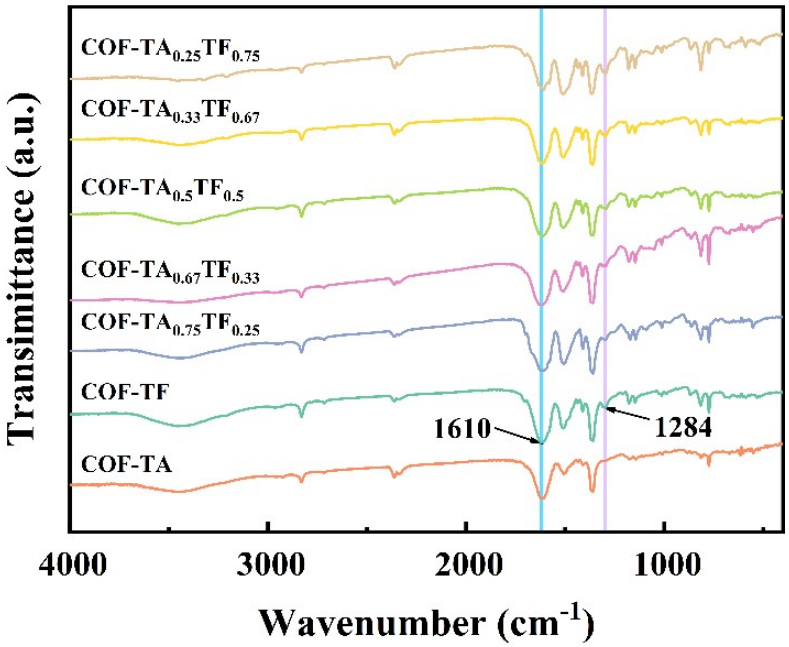

Fig. S3. FTIR spectra of COF-TA, COF-TF and COF-TA_aTF_b (a+b = 1, a = 0.75, 0.67, 0.50, 0.33, 0.25).

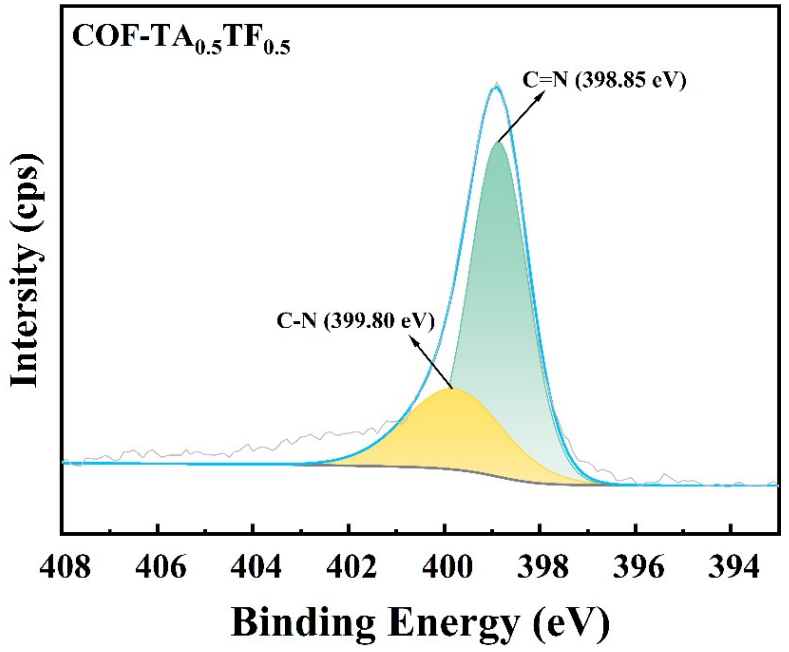

Fig. S4. The XPS fitting plot of COF-$TA_{0.5}TF_{0.5}$ for N 1s.

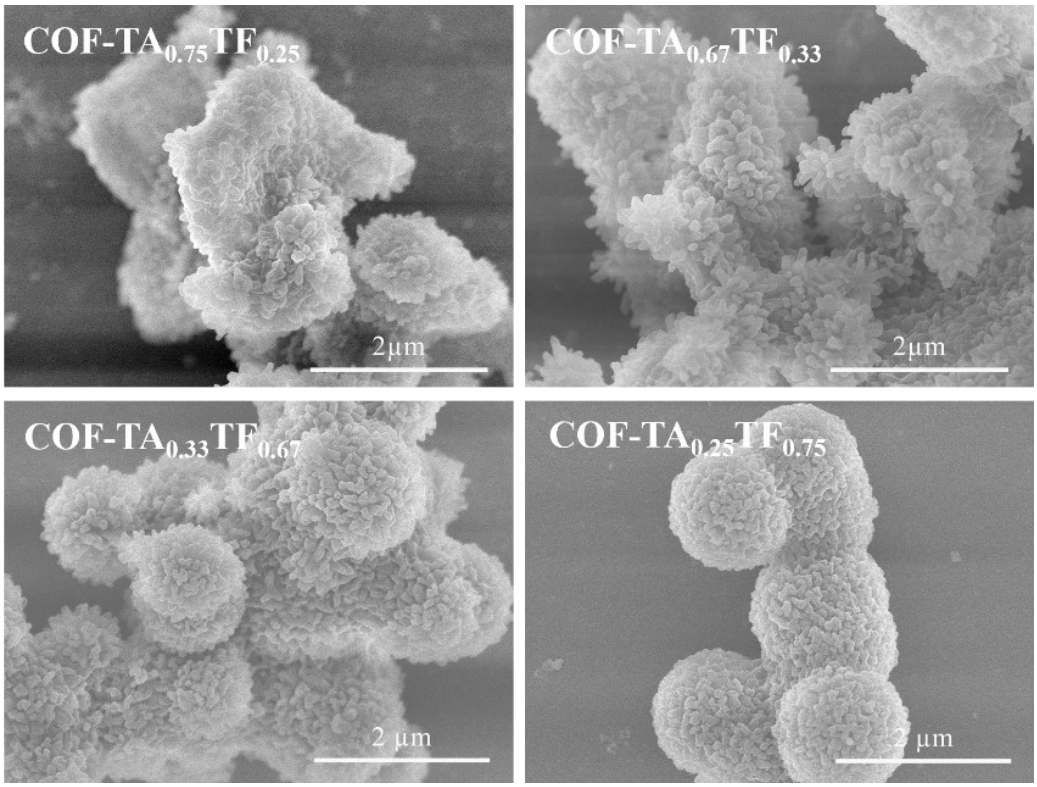

Fig. S5. SEM images of COF-$TA_{0.75}TF_{0.25}$, COF-$TA_{0.67}TF_{0.33}$, COF-$TA_{0.33}TF_{0.67}$ and COF-$TA_{0.25}TF_{0.75}$.

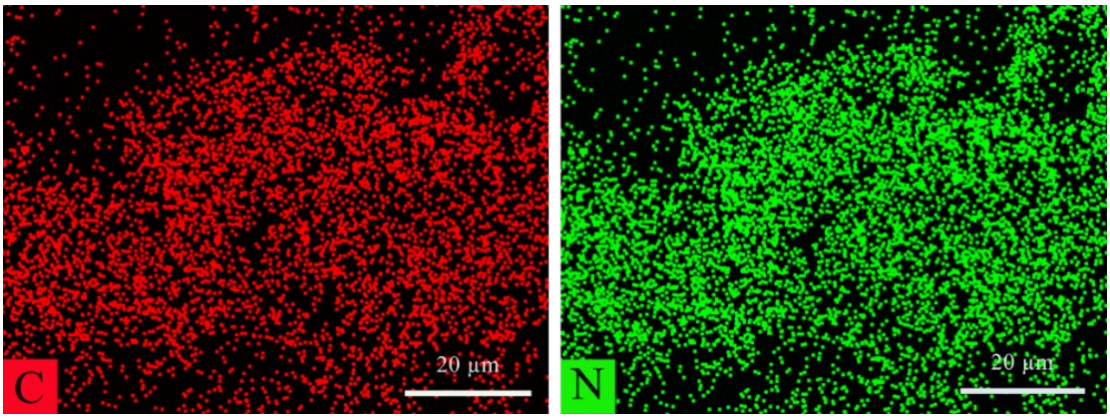

Fig. S6. SEM-EDX of COF-TA.

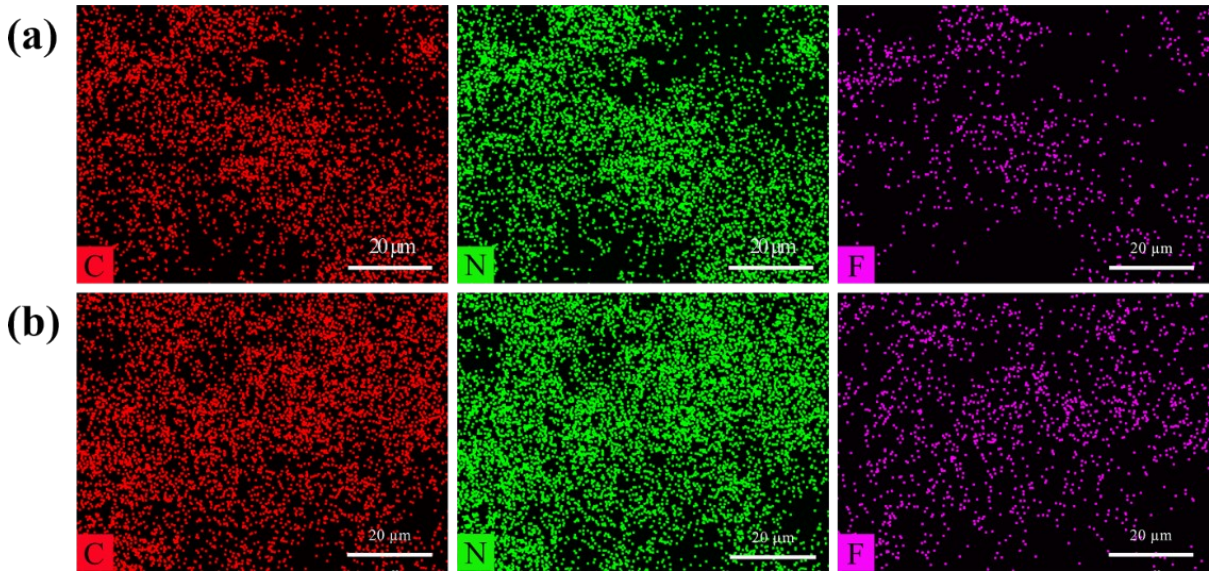

Fig. S7. SEM-EDX of (a) COF-$TA_{0.75}TF_{0.25}$ and (b) COF-$TA_{0.67}TF_{0.33}$.

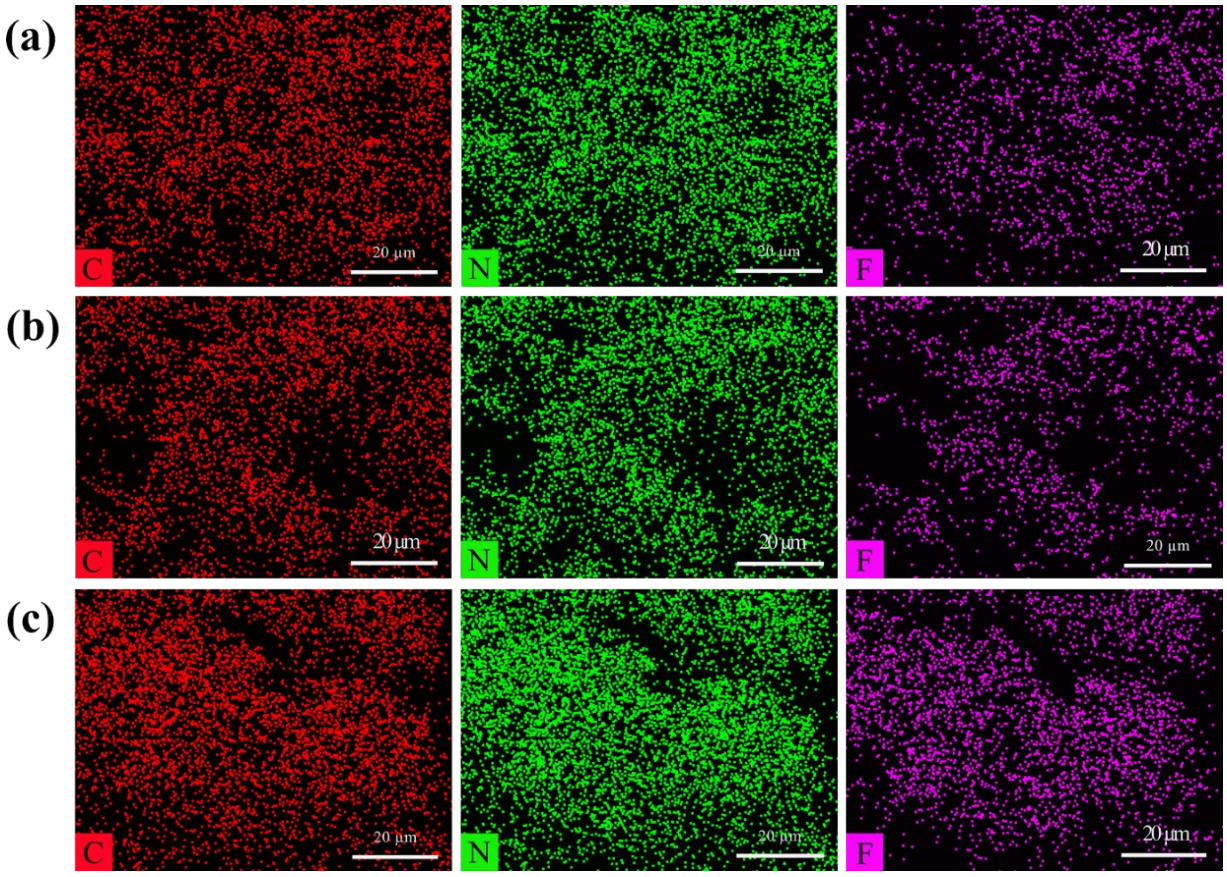

Fig. S8. SEM-EDX of (a) COF-$TA_{0.33}TF_{0.67}$, (b) COF-$TA_{0.25}TF_{0.75}$ and (c) COF-TF.

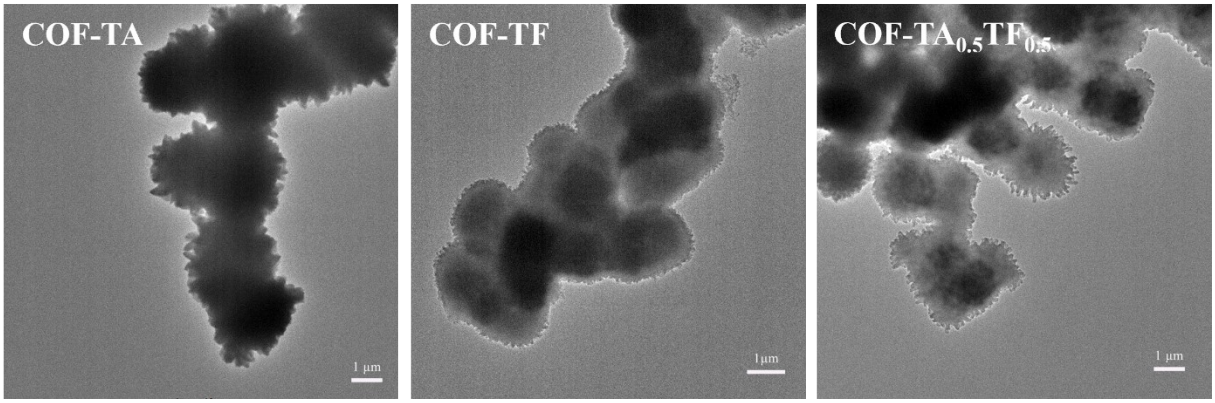

Fig. S9. TEM images of COF-TA, COF-TF and COF-$TA_{0.5}TF_{0.5}$.

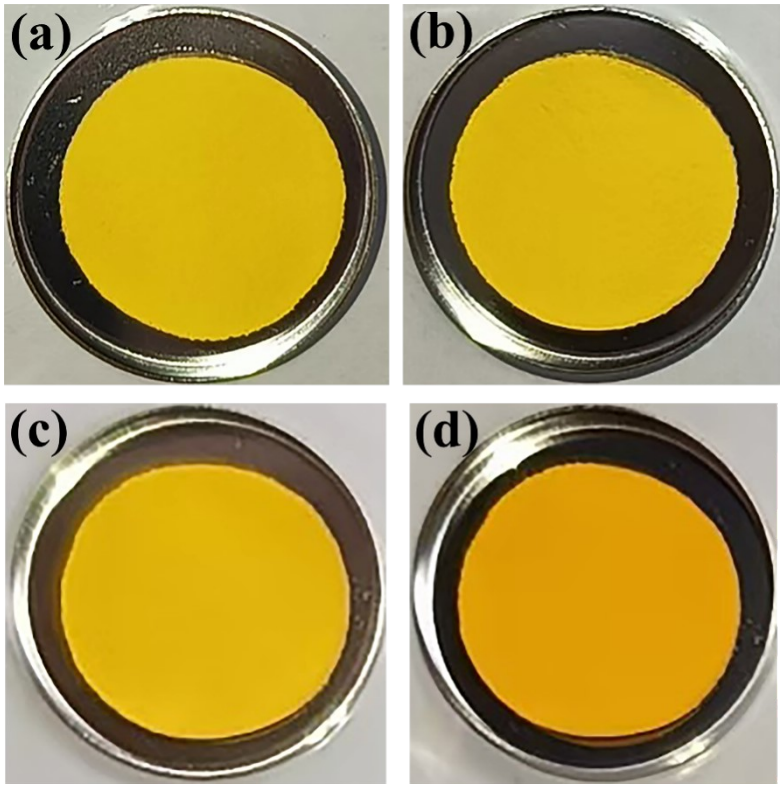

Fig. S10. Photographs of the COF-$TA_{0.5}TF_{0.5}$ electrolyte membrane after being stored in an electric blast drying oven for 1 h at different temperatures: (a) 60 °C, (b) 100 °C, (c) 140 °C and (d) 180 °C.

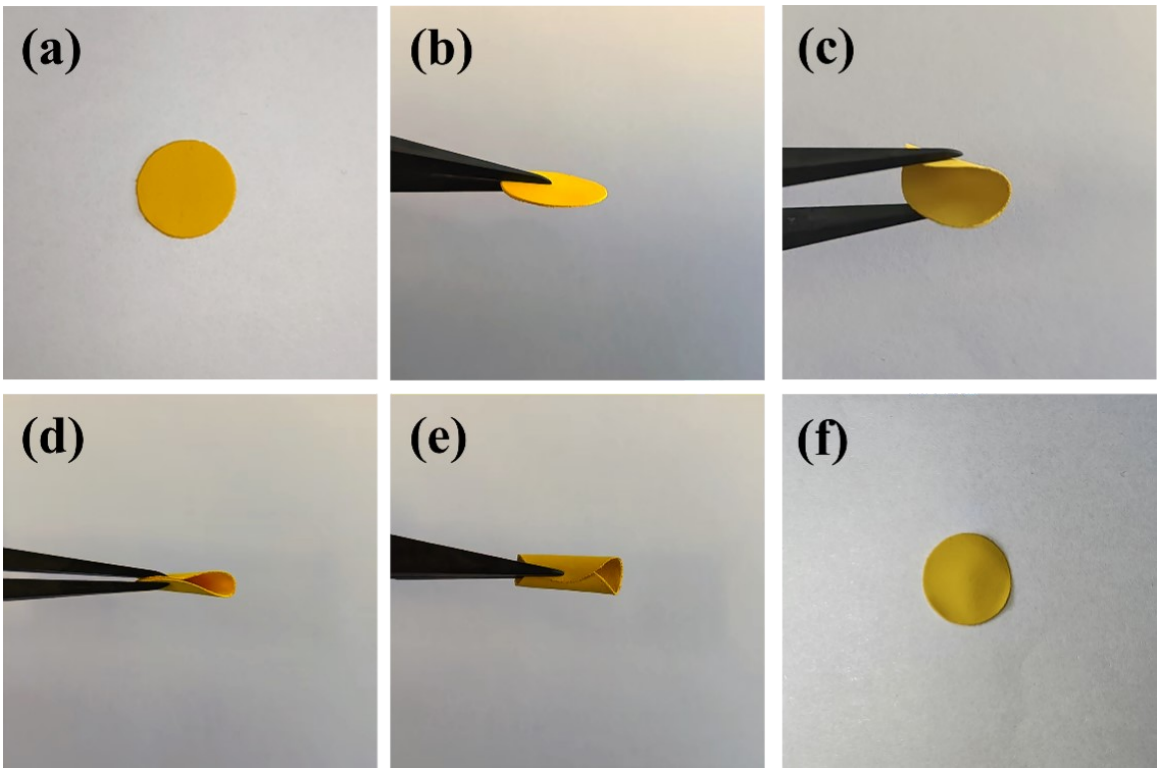

Fig. S11. Optical photo of COF-$TA_{0.5}TF_{0.5}$ quasi-solid-state electrolyte membrane.

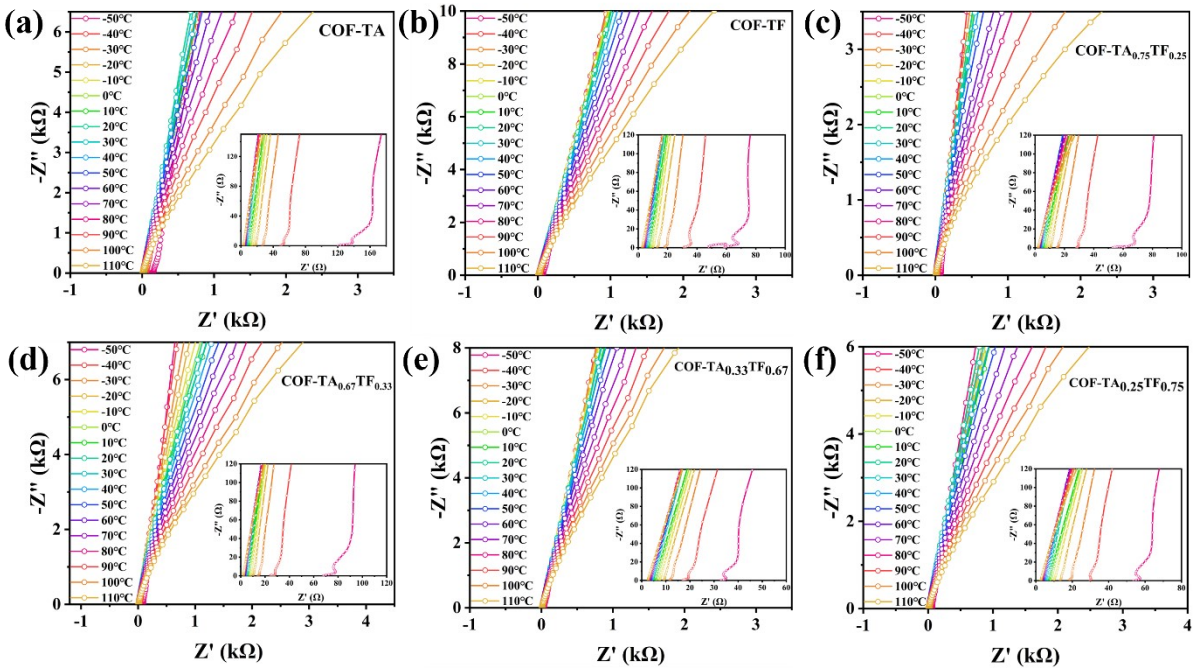

Fig. S12. Typical Nyquist plots of the ss|QSSEs|ss cell at various temperatures from −50 °C to 110 °C (the internal is the magnified high frequency area) of (a) COF-TA, (b) COF-TF, (c) COF-$TA_{0.75}TF_{0.25}$, (d) COF-$TA_{0.67}TF_{0.33}$, (e) COF-$TA_{0.33}TF_{0.67}$ and (f) COF-$TA_{0.25}TF_{0.75}$.

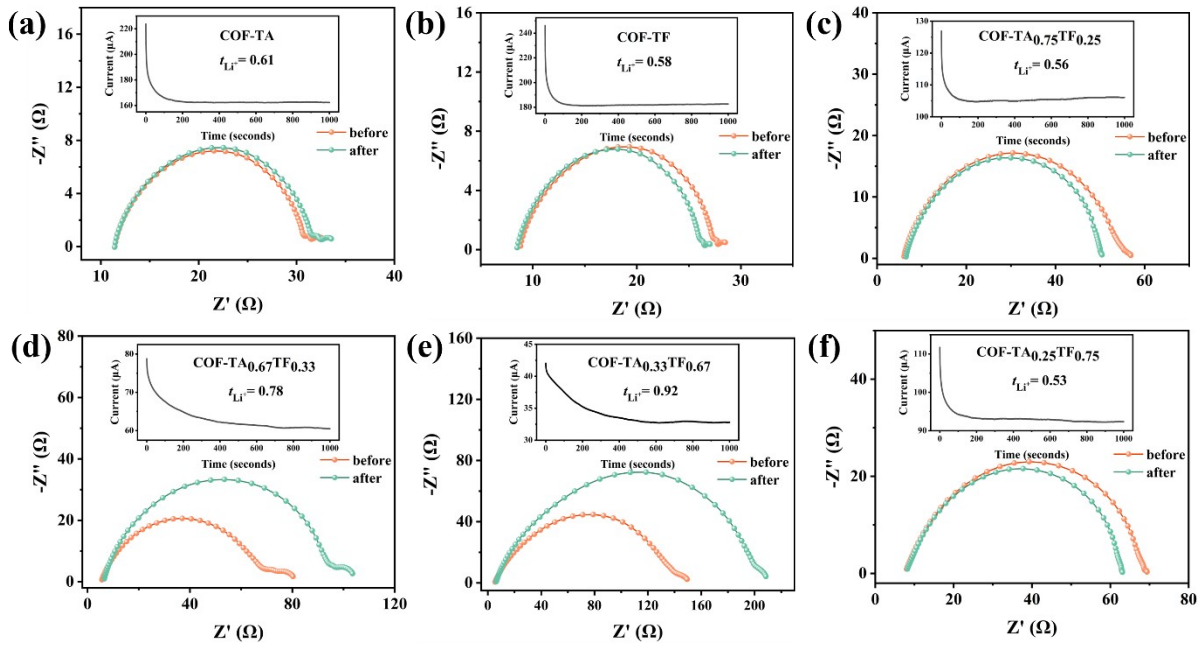

Fig. S13. Chronoamperometric curves and EIS curves of (a) COF-TA, (b) COF-TF, (c) COF-$TA_{0.75}TF_{0.25}$, (d) COF-$TA_{0.67}TF_{0.33}$, (e) COF-$TA_{0.33}TF_{0.67}$ and (f) COF-$TA_{0.25}TF_{0.75}$ electrolyte before and after polarization.

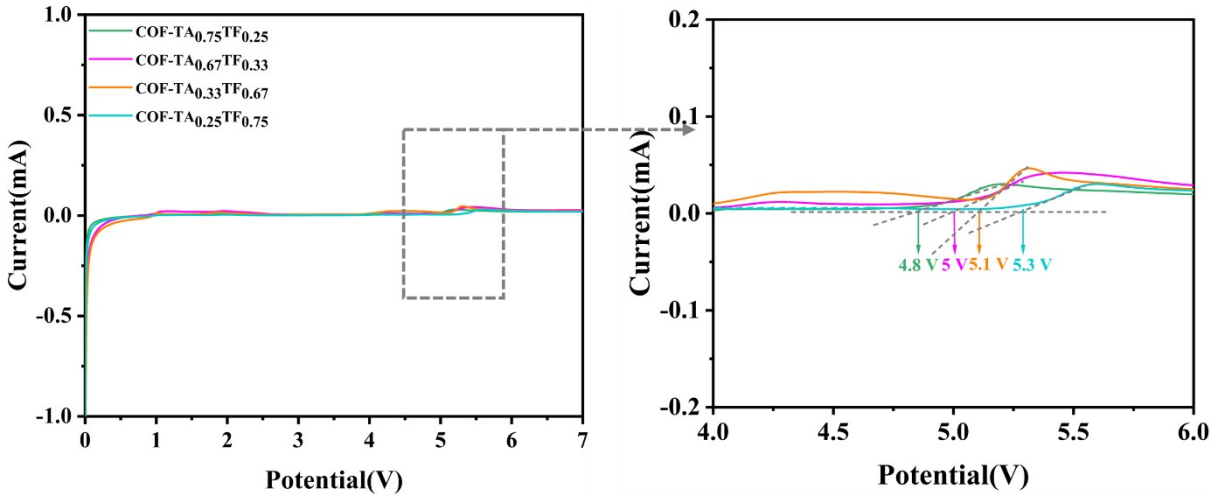

Fig. S14. The LSV curves of COF-$TA_{0.75}TF_{0.25}$, COF-$TA_{0.67}TF_{0.33}$, COF-$TA_{0.33}TF_{0.67}$ and COF-$TA_{0.25}TF_{0.75}$ electrolyte at room temperature.

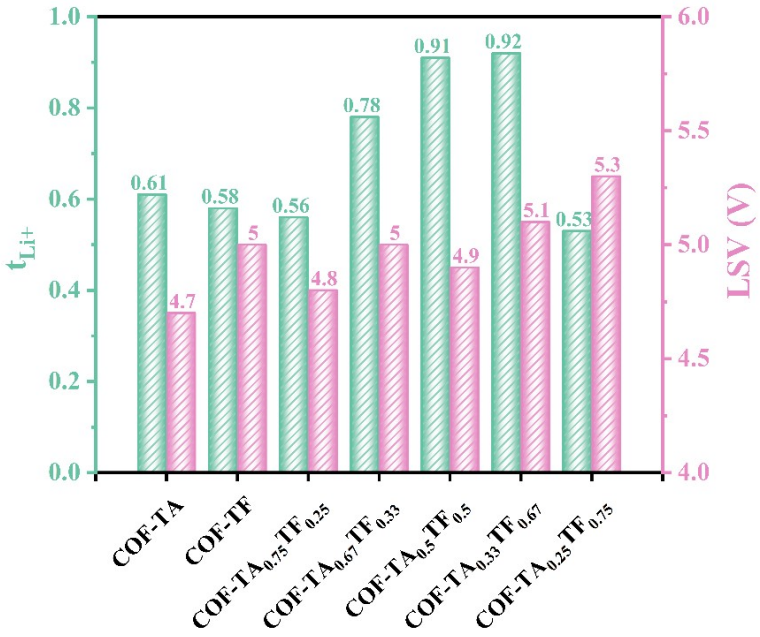

Fig. S15. The comprehensive t_{Li^+} and LSV comparison of COF-TA_aTF_b (a+b = 1, a = 0.75, 0.67, 0.5, 0.33, 0.25) QSSE.

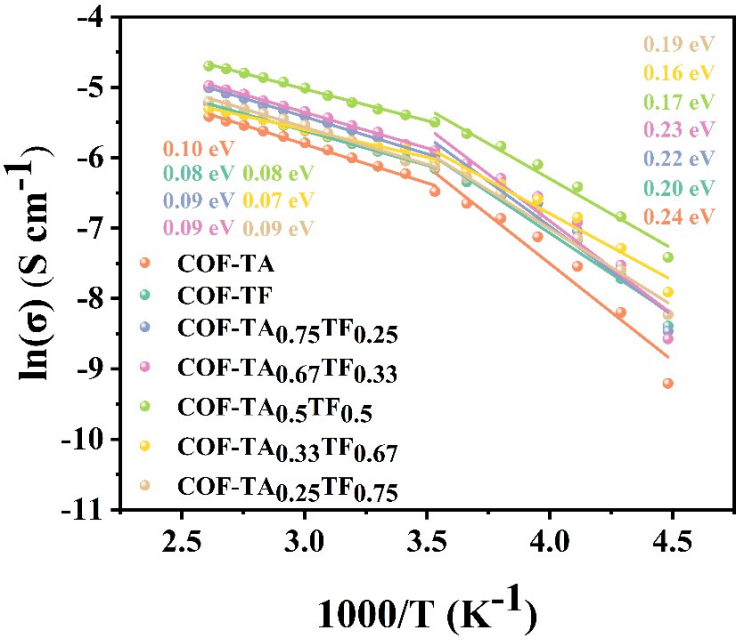

Fig. S16. Arrhenius plots of different QSSEs.

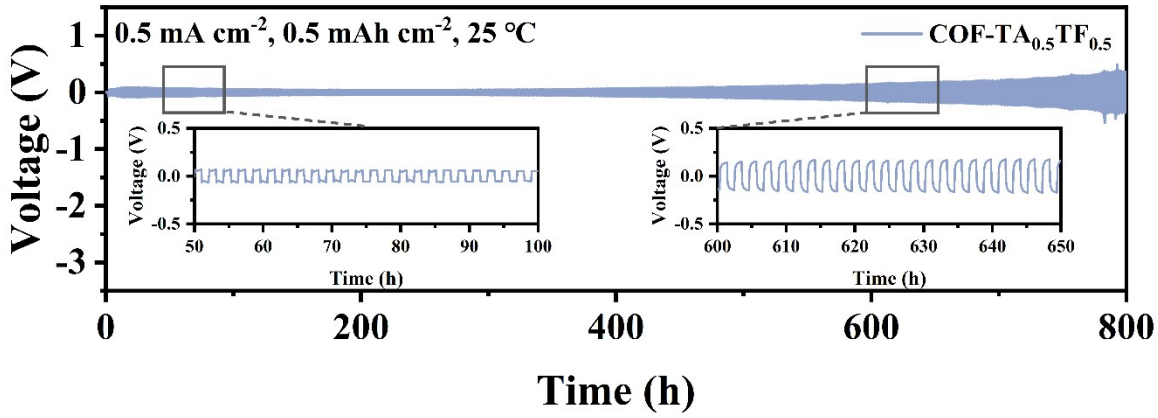

Fig. S17. Voltage profiles of the Li|COF-$TA_{0.5}TF_{0.5}$|Li symmetric cells with a current density of 0.5 mA cm^{-2} at room temperature.

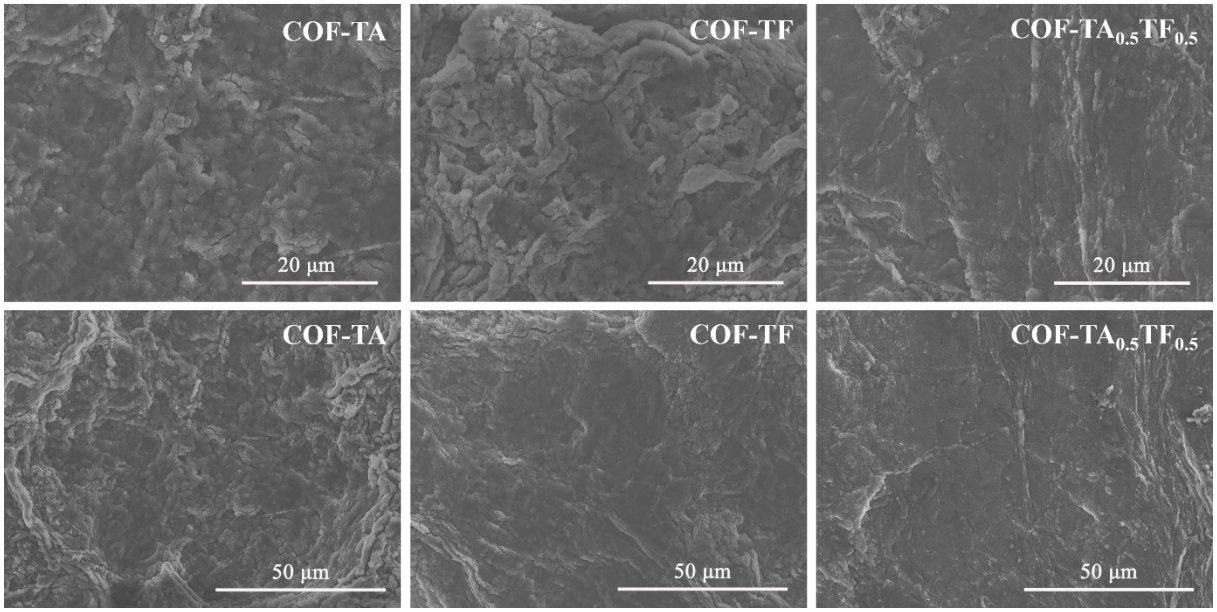

Fig. S18. SEM images of Li foil from Li symmetric cells with COF-TA, COF-TF and COF-$TA_{0.5}TF_{0.5}$ after the lithium plating/stripping at the current density of 0.1 mA cm^{-2} and the capacity of 0.1 mAh cm^{-2}, respectively.

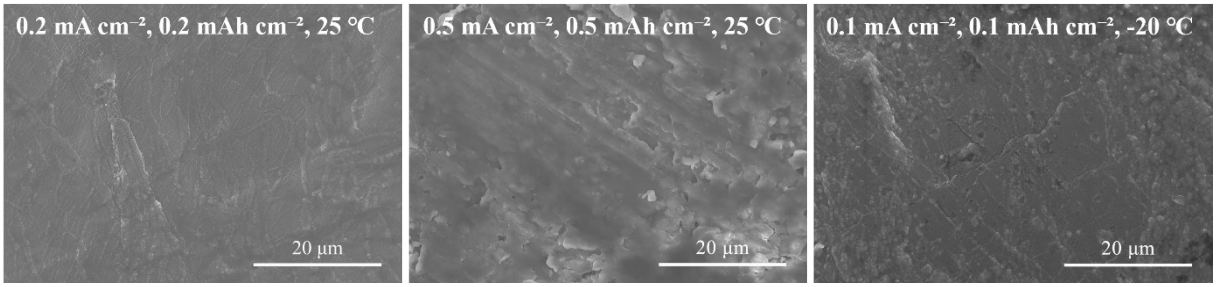

Fig. S19. SEM images of Li foil from Li symmetric cells with COF-$TA_{0.5}TF_{0.5}$ after the lithium plating/stripping at varying current densities, the capacities and temperatures.

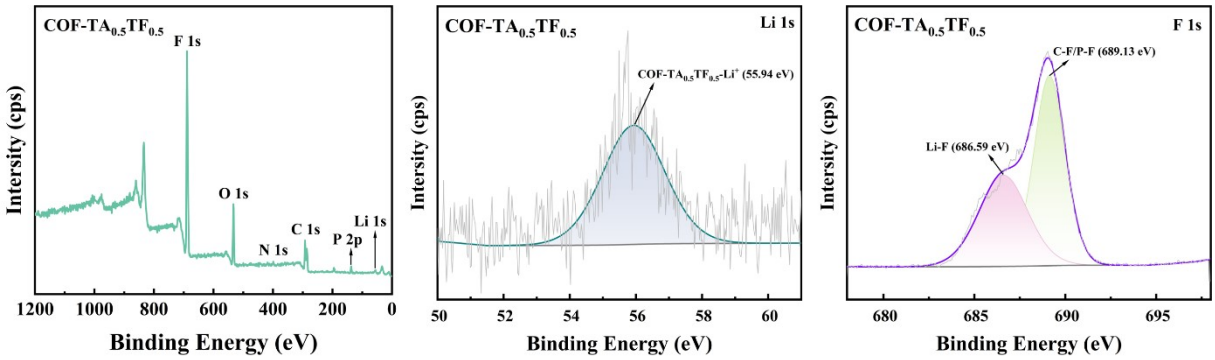

Fig. S20. XPS survey spectrum of COF-$TA_{0.5}TF_{0.5}$; the XPS fitting plot of COF-$TA_{0.5}TF_{0.5}$ after the lithium plating/stripping at the current density of 0.2 mA cm^{-2} and the capacity of 0.2 mAh cm^{-2} for Li 1s and F 1s, respectively.

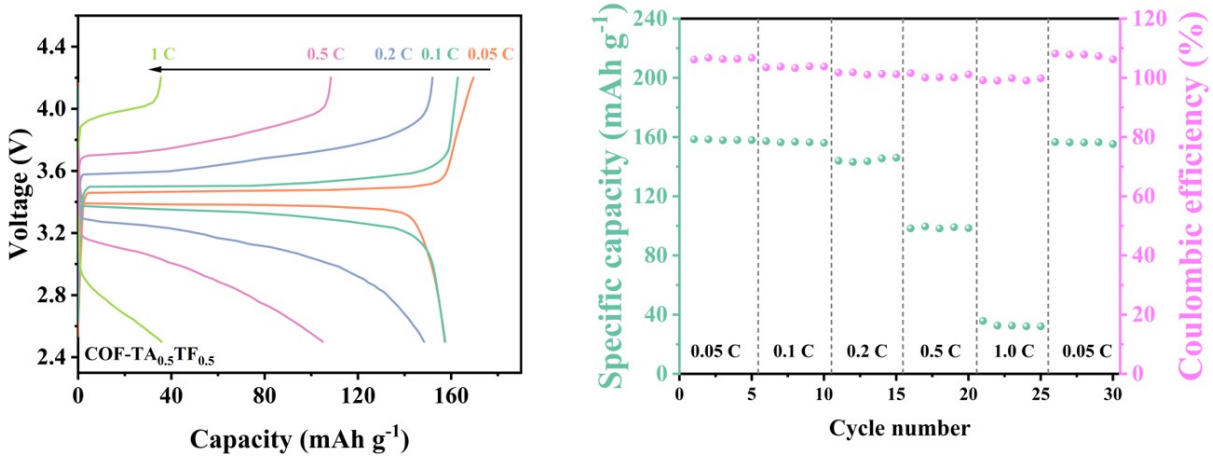

Fig. S21. Charge and discharge voltage profiles of COF-$TA_{0.5}TF_{0.5}$ at different rates; Rate performance of QSSE with COF-$TA_{0.5}TF_{0.5}$.

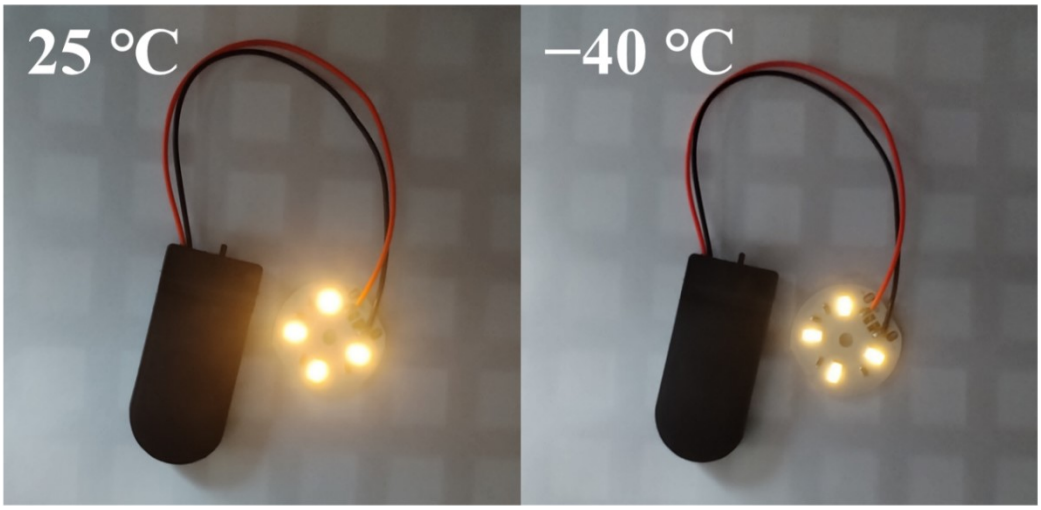

Fig. S22. Photographs showing the bulb being lit by LFP|COF-$TA_{0.5}TF_{0.5}$|Li at room temperature and −40 °C, respectively.

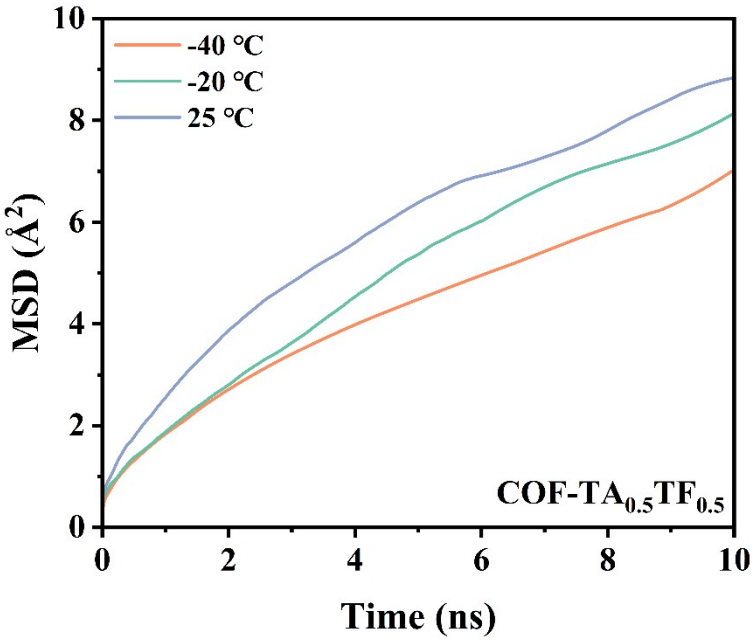

Fig. S23. Calculated mean square displacement (MSD) of Li^+ in electrolytes as a function of the simulation time.

Table S1. ICP-OES results of COF-TA, COF-$TA_{0.5}TF_{0.5}$ and COF-TF.

Samples	Li/wt.%	Li/mg	$LiPF_6$/mg
COF-TA	2.01	0.80	17.61
COF-$TA_{0.5}TF_{0.5}$	2.26	0.90	19.80
COF-TF	2.05	0.82	17.93

Table S2. The ionic conductivity summery of COF-TA, COF-TF, COF-$TA_{0.75}TF_{0.25}$, COF-$TA_{0.67}TF_{0.33}$, COF-$TA_{0.5}TF_{0.5}$, COF-$TA_{0.33}TF_{0.67}$, COF-$TA_{0.25}TF_{0.75}$ at different temperatures.

	σ (mS cm^{-1})						
Temperature	**COF-TA**	**COF-TF**	**COF-$TA_{0.75}TF_{0.25}$**	**COF-$TA_{0.67}TF_{0.33}$**	**COF-$TA_{0.5}TF_{0.5}$**	**COF-$TA_{0.33}TF_{0.67}$**	**COF-$TA_{0.25}TF_{0.75}$**
–50 °C	0.1	0.227	0.211	0.189	0.601	0.367	0.267
–40 °C	0.275	0.446	0.466	0.539	1.07	0.686	0.502
–30 °C	0.529	0.779	0.872	0.991	1.64	1.06	0.793
–20 °C	0.805	1.11	1.30	1.43	2.25	1.38	1.11
–10 °C	1.05	1.44	1.68	1.85	2.92	1.71	1.49
0 °C	1.30	1.76	2.07	2.28	3.49	2.05	1.86
10 °C	1.54	2.12	2.50	2.74	4.10	2.37	2.17
20 °C	1.98	2.43	2.80	2.99	4.55	2.82	2.36
30 °C	2.20	2.71	3.30	3.56	4.93	2.90	2.76
40 °C	2.47	3.03	3.65	3.92	5.44	3.11	3.14
50 °C	2.76	3.33	4.06	4.36	5.98	3.39	3.53

60 °C	3.06	3.63	4.48	4.77	6.67	3.65	3.94
70 °C	3.35	3.92	4.85	5.16	7.25	3.97	4.32
80 °C	3.62	4.27	5.23	5.56	7.73	4.29	4.65
90 °C	3.92	4.60	5.75	6.12	8.25	4.54	4.97
100 °C	4.17	4.94	6.20	6.50	8.76	4.77	5.24
110 °C	4.45	5.31	6.68	6.90	9.11	4.95	5.51

Table S3. The Li^+ conductivity comparison between COF-$TA_{0.5}TF_{0.5}$ and reported work previously in wide temperature range.

NO.	Materials	σ (mS cm^{-1})	t_{Li^+}	temperature range (°C)	E_a (eV)	Reference
1	$LiBF_4$/PC@PBI-COF	1.87 (30 °C) 3.94 (85 °C)	0.58	30-85	0.18 (30-85 °C)	1
2	G_4Li@COF	0.165 (25 °C)	0.80	20-80	0.35 (20-80 °C)	2
3	CF_3-COF@PVDF-HFP	1.21 (25 °C)	0.77	-	-	3
4	3D-SpCOF-OH	1.3 (25 °C)	0.64	25-80	0.03 (VTF)	4
5	TpDa-Li COF	0.925 (25 °C)	0.89	25-85	0.20 (25-85 °C)	5
6	COF_{ds}	0.101 (25 °C)	0.91	30-80	0.14 (30-80 °C)	6
7	PEO-Li^+@N-COF	0.24 (60 °C)	0.76 (60 °C)	40-70	0.45 (40-70 °C)	7

8	dCOF-ImTFSI-60@Li	0.0974 (30 °C) 7.05 (150 °C)	0.72	30-150	0.28 (30-150 °C)	8
9	LiOOC-COF3	0.0136 (30 °C) 0.11 (80 °C)	0.91	30-80	0.17 (30-80 °C)	9
10	FPI-COF	0.33 (25 °C)	0.82	25-70	0.14 (25-70 °C)	10
11	COF-MCMC	0.49 (30 °C)	0.71	–20-60	0.31 (–20-60 °C)	11
12	Li^+-PEG@NUST-23	0.0710 (0 °C) 1.36 (80 °C)	-	-	-	12
13	COF-SS-Li	0.0963 (20 °C) 0.128 (40 °C) 0.552 (100 °C)	0.53	20-100	0.24 (20-100 °C)	13
14	Li^+@Crown-COF	3.5 (30 °C) 5.6 (60 °C) 8.5 (80 °C)	0.60	30-80	0.13 (30-80 °C)	14
15	CSQ-COF-2	0.727 (80 °C)	0.83	30-80	0.12 (30-80 °C)	15
16	ETPTA-COF-S	1.29 (20 °C)	0.83	20-60	0.21 (20-60 °C)	16

17	LITFSI@EO-BIm-iCOF	0.108 (25 °C)	0.69	25-85	0.19 (25-85 °C)	17
18	PEO-TB-COF	0.889 (25 °C)	0.80	25-85	0.185 (25-85 °C)	18
19	**COF-$TA_{0.5}TF_{0.5}$**	**1.07 (–40 °C)** **4.75 (25 °C)** **9.11 (110 °C)**	**0.87 (–40 °C)** **0.79 (–20 °C)** **0.91 (25 °C)**	**−50-110**	**0.17 (−50-10 °C)** **0.08 (10-110 °C)**	**This work**

Table S4. The cycling performances comparison between COF-$TA_{0.5}TF_{0.5}$ and other similar COF-based electrolytes reported previously.

NO.	Materials	System	Cycle rate	Temperature (°C)	Coulombic effciency	Reference
1	Li^+-PEG@NUST-23	$LiFePO_4$/Li	0.1 C	10	97.82 (80 cycles)	12
2	$BtCOF_{2\%}$-SPE	$LiFePO_4$/Li	0.1 C	25	86.6 (200 cycles)	19
3	Dha-COF_{im}-IL	$LiFePO_4$/Li	0.1 C	25	90 (80 cycles)	20
4	COF-ECJTU1-60-SO_3Li	$LiFePO_4$/Li	0.2 C	30	99.1 (40 cycles)	21
5	**COF-$TA_{0.5}TF_{0.5}$**	**$LiFePO_4$/Li**	**0.1 C**	**25** **−20**	**99.36 (130 cycles)** **99.80 (100 cycles)**	**This work**

References

1. H. Zhang, Y.-R Kong, J. Zhang, X. Y. Ren and X. M. Ren, *J. Mater. Chem. C* 2023, **11**, 14336.
2. C. Song, Y. Zhao, Y. W, D. Yan, Y. Cai, Y. Zhang, W. Luo, K. Awaga and Y. Wang, *Energy Storage Mater.* 2025, **80**, 104424.
3. G. Feng, Q. Ma, D. Luo, T. Yang, Y. Nie, Z. Zheng, L. Yang, S. Li, Q. Li, M. L. Jin, X. Wang and Z. Chen, *Angew. Chem. Int. Ed.* 2025, **64**, e202413306.
4. S. Wang, X. Li, T. Cheng, Y. Liu, Q. Li, M. Bai, X. Liu, H. Geng, W.-Y. Lai and W. Huang, *J. Mater. Chem. A* 2022, **10**, 8761.
5. C. Wang, P. Shi, H. Zhang, Y. Zhang, Y. Gao, *Int. J. Hydrogen Energy* 2024, **73**, 443.
6. R. H. Choi, A. Gurumoorthi, S. Bae, C. Y. Son and H. R. Byon, *Adv. Energy Mater.* 2025, e04143.
7. D. Shen, W. Liang, X. Wang, L. Yue, B. Wang, Y. Zhou, Y. Yu and Y. Li, *Energy Storage Mater.* 2024, **72**, 103709.
8. Z. Li, Z. W. Liu, Z. Li, T. X. Wang, F. Zhao, X. Ding, W. Feng and B. H. Han, *Adv. Funct. Mater.* 2020, **30**, 1909267.
9. G. Zhao, Z. Mei, L. Duan, Q. An, Y. Yang, C. Zhang, X. Tan and H. Guo, *Carbon Energy*. 2023, **5**, e248.
10. D.-H. Guan, X.-X. Wang, L. Li, G.-N. Chen, G.-Y. Qiao and J.-J. Xu, *J. Am. Chem. Soc.* 2025, **147**, 38078.
11. W. Gong , Y. Ouyang, S. Guo, Y. Xiao, Q. Zeng, D. Li, Y. Xie, Q. Zhang and S. Huang, *Angew. Chem. Int. Ed.* 2023, **62**, e202302505.
12. Y. Xuan, Y. Wang, B. He, S. Bian, J. Liu, B. Xu and G. Zhang, *Chem. Mater.* 2022, **34**, 9104.
13. J. Zhang, D. Luo, H. Xiao, H. Zhao, B. Ding, H. Dou and X. Zhang, *ACS Appl. Mater. Interfaces* 2023, **15**, 34704.
14. M. Gu, J. Wu, C. Li, Z. Zhang, Y. Wu, X. Cheng, R. Li, Y. Tian, K.-T. Bang, R. Wang, S. Suleman, Y. Yuan, J. Huang, D.-M. Shin, Z.-L. Xu, Y. Wang and Y. Kim, *Adv. Mater.* 2025, e11473.
15. Y. Xue, Q. Lin, X. Sun, D. Li, Y. Fu, Z. Li, Y. Shi, C. Luo, X. Gui and K. Xu, *Small* 2025, **21**, 2501988.
16. X. Zhuang, Y. Hui, Y. Feng, J. Chen, J. Chen and Y. Wang, *Sci China Chem*, 2025, **68**, 1533.
17. J. Song, L. Lin, F. Cui, H.-G. Wang, Y. Tian and G. Zhu, *Chem. Sci.* 2024, **15**, 11480.

18 Y. Zhang, C. Shan, Z. Chen, S. Wang, C. Wei, Y. Tian, X. Jin, Y. Zhao, X. Liu, Y. Wang and W. Huang, *Small* 2025, **21**, 2502407.

19. X. Tan, Y. Tong, J. Yang, X. Du, A. Yang, A. Zhang and Q. Xu, *Polym. Chem.* 2025, **15**, 454-464.

20. X. Tan, J. Zhong, Y. Tong, L. Guo, Y. Xie and J. Zhao, *Polymer.* 2025, **317**, 127911.

21. S. Mi, Y. Geng, Y. Wang, C. Wang, Z. Yang, F. Zhao and Z. Li, *Small* 2025, **21**, e07272.